

Geochemical Modeling and Experimental Studies on Mineral Carbonation of Primary Silicates for Long-term Immobilization of CO₂ in Basalt from the Eastern Deccan Volcanic Province

J. P. Shrivastava*, N. Rani and V. Pathak

Department of Geology, University of Delhi, Delhi, India

*Corresponding Author: jpsrivastava.du@gmail.com

ABSTRACT

Deccan flood basalt records immense accumulation (1.5 X 10⁶ km² area) of tholeiitic magma in a relatively short time span. For mineral carbonation study and long-term storage of CO₂, massive tholeiitic basalt from the Mandla lobe of the eastern Deccan volcanic province was considered as it contains a high amount of reactant minerals such as Ca, Mg and Fe rich silicates. Main objective of the present study is to understand effects of CO₂ concentration on conversion of Ca, Mg and Fe bearing silicate minerals in to stable carbonate minerals such as calcite, dolomite, magnesite and siderite. Computer based computation details of chemistry of basalt-water-CO₂ interaction, under laboratory induced hydrothermal-like conditions, form the basis of the treatment of basalt specimens. Grain surface area value = 23,000 cm²/g was maintained throughout the experiments. A series of experiments were performed at accelerated conditions of 5 and 10 bars pCO₂, while vessel pressures were maintained at 10 and 20 bars at 100 and 200 °C temperatures for 50, 60, 70 and 80 hours, respectively. XRD and SEM-EDS results show presence of calcite (Ca_{0.29} C_{0.79} O₆), aragonite (Ca_{0.43} C_{1.19} O₉), siderite (Fe_{0.45} C_{0.79} O₆) and magnesite (Mg_{0.11} C_{0.79} O₆) in the treated samples. It is also observed that mineral carbonation accompanied by dissolution reactions led to rise in the pH (7.42) of the solution, when treated for 80 hours at 100 °C temperature and 5 bar pCO₂ pressure. A sudden decrease in the pH (6.85) is also noticed in case of a specimen treated similarly, but at elevated (10 bar) pCO₂. Bulk of the neo-formed secondary product is mainly composed of clay minerals. Present experimental results correspond largely to those obtained from kinetic modelling of basalt-water-CO₂ interaction. Results indicate presence of similar carbonate minerals such as calcite, aragonite, siderite and magnesite. Details pertaining to mineral carbonation related phase transformations are discussed in the paper.

INTRODUCTION

Carbon dioxide is one of the most important green house gases in Earth's atmosphere. Changes in pCO₂ concentration have significant effects on the surface temperature of the Earth (Houghton and Wood, 1987), which leads to major deviation in the climate, surface processes and biota. Marini (2007) had stated that soon after the onset of the industrial revolution, atmospheric CO₂ concentration increased considerably with time (for the past 45-50 a.) attaining anomalous values (e. g. Oelkers and Cole, 2008 - CO₂ concentration in Earth's atmosphere has increased from ~ 325 ppm in 1970 to 380 ppm at the beginning of this century). Rochelle et al., (2004) have discussed a variety of CO₂-water-rock chemical reactions to safely trap CO₂, suitable for geological time-scales. Geologic storage (Bachu and Adams, 2003; IPCC, 2005) and other options of CO₂ sequestration were exercised in the past (Brennan and Burruss, 2003; Xu et al., 2005) to reduce CO₂ emissions (Metz et al., 2005). Massive basalt flows contain abundant Ca-Mg-Fe rich silicate minerals (occur all around the world). They play a significant role in the global carbon cycle (Brady and Gislason, 1997; Retallack, 2002). Large igneous provinces such as continental flood

basalts, volcanic passive margins and oceanic plateaus (Best, 2001) represent immense accumulation of mafic (Fe and Mg rich) magmas. Presence of abundant quantities of olivine, pyroxene and plagioclase (that are rich in Mg or Fe or Ca contents, respectively) were reported (Ahmad, 2002) from Mandla lavas. They provide a suitable matrix for CO₂ sequestration. Charan et al., (2010) have suggested suitability of the Igatpuri picritic basalt flows for CO₂ sequestration. Holloway et al., (2008) have stated that India has potential sites for large scale geological CO₂ storage. Conversion of CO₂ gas into stable carbonate minerals such as calcite, dolomite, magnesite and siderite is considered as one of the best options for long-term storage of CO₂ (Oelkers et al., 2008). Studies by Broecker (2008), on capturing and storing of CO₂, have revealed that the layered basalt provinces such as Deccan Traps in India (Fig. 1) offer large area storage depot for captured CO₂. However, such possibilities are yet to be tested in detail.

To predict or model long-term CO₂ sequestration in Deccan basalts, mineral carbonation mechanism requires to be quantified by resolving key parameters, such as pCO₂ (in ppmv), temperature and time. The main objective of the present study is aimed at in better understanding of silicate mineral carbonation reactions under natural and laboratory

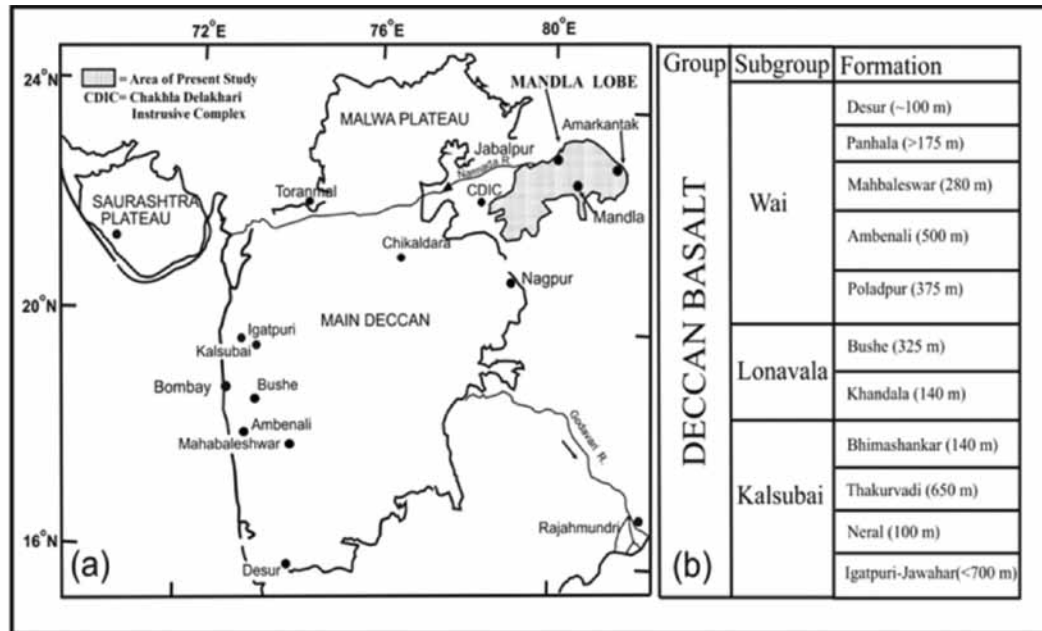


Figure 1. Map showing outcrop of the Deccan volcanic province and location of the Mandla lobe (with grey shade) of the eastern Deccan volcanic province, and (b) stratigraphic succession of the western Deccan province.

induced accelerated pressure and temperature conditions. These reactions between CO₂ and primary silicate minerals such as olivine, pyroxene and plagioclase (as reactants) and secondary carbonates help to understand the rate and extent of mineral carbonation. The resultant pathways will be utilized in understanding the reactive phases suitable for mineral trapping of supercritical CO₂ reactions under variable P, T, S/V, porosity and permeability conditions.

MANDLA LOBE: A LABORATORY FOR CO₂ SEQUESTRATION

The Mandla lobe, an isolated, large (29,351 km²) north-eastern outlier of the Deccan Traps, extends E-W for 344 km and 156 km N-S around the towns of Seoni, Jabalpur, Mandla, Dindori and Amarkantak areas (Fig. 2). The landscape is covered with flat-topped plateaus (commonly known as *macula plateau*) and ridges that often contain small mesas and buttes. Major topographic breaks occur at elevations of about 450, 600 and 900 m a. s. l. (Fig. 2), where duricrusts of laterite often cap the plateau above these breaks and provide several stratigraphically important lava flow exposures of the lava pile. Tholeiitic lava flows from the Mandla lobe of the eastern Deccan basalt province are considered in the present study because of their large and continuous areal extent, large combined thickness of the flows (>1 km in some localities), inter and intra-flow features, abundance of reactive silicate minerals and Mesozoic sediments containing Fe-Mg-Ca silicate minerals. On the basis of regional mapping, physical characters, petrography and lateral tracing of the lava

flows, Pattanayak and Shrivastava (1999) have recorded the presence of thirty-seven lava flows in the ~ 900 m thick volcano-sedimentary sequences around Mandla. These were characterized further by their major element chemistry (Shrivastava and Pattanayak, 2002). Major-oxide chemistry was used for further grouping them in to eight chemical types (Shrivastava and Ahmad, 2005a). Modal data for each of the mineral phases and glass show vast variability in the modal percentages of pyroxene (65.31-18.27 %) and plagioclase (47.00-19.00 volume %), though, these flows contain < 8.29 % olivine and the subordinate amount of Fe oxide and glass. Distribution of cations on M₁ and M₂ sites, together with Mg: Fe: Ca ratios for pyroxenes show presence of Ca-rich and Ca-poor pyroxenes; however the later type of the pyroxene present in this area is either Fe-rich or Fe-poor in composition. The Ca-poor, but Fe-rich pyroxenes (Ca: Mg: Fe = 24: 22: 54 and 22: 14: 64, respectively) are associated with the commonly found high diopside and olivine normative tholeiitic lava flows. Most of the Ca rich microphenocrysts are mainly ferro-augite. Sub-calcic augite and pigeonite are also common in this area. The Fe rich mineral phases in lava flows are mainly ilmenite-magnetite, olivine and pyroxenes. The Fe/Fe+Mg for pyroxene (both phenocrysts and microphenocrysts), olivine and whole rock data show wide variation. Distribution of cations in W and Z sites of the plagioclase structure and Na (as Ab): Ca (as An): and K (as Or) ratio when calculated for the Mandla lavas show poor An content in the plagioclase reflecting a more sodic composition. The co-existing magnetite-ilmenite in 37 lava flows represent a wide variation in their FeO (47.14-

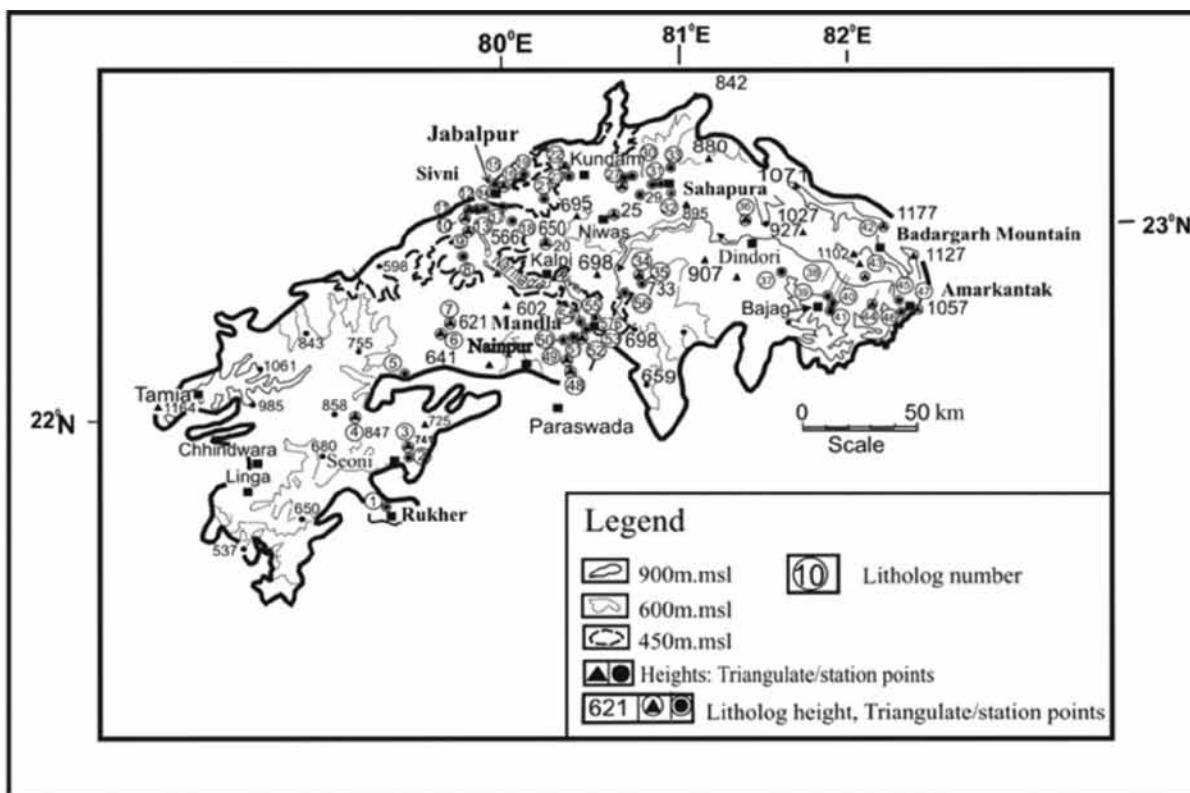


Figure 2. Map showing topographic details of the area of study - Mandla lobe of the eastern Deccan volcanic province

56.59), Fe₂O₃ (14.41-38.44) and TiO₂ contents (Ahmad and Shrivastava, 2004). Combined trace elemental and isotopic compositions for basaltic lava flows of the Mandla lobe show chemical affinities with Poladpur, Mahabaleshwar and Ambenali formation basalts of the distant south-western Deccan volcanic province (Shrivastava et al., 2014).

CARBONATE FACIES: EVIDENCE OF GEOLOGICAL SEQUESTRATION OF CO₂

Sufficiently thick, sedimentary carbonate units (sandwiched between lava flows), developed in the hiatuses between two successive eruptive events suggest relatively less violent eruptive activity in Mandla area as compared to those that occurred in its western counterpart. In this area, significantly thick limestone and inter-calcareous lithofacies constitute major part of the infra/inter-traps (Fig. 3). It contains a variety of carbonate lithologies - limestone, brecciated calcrete, calcareous siltstone with calcareous nodules, nodular and pisolitic calcrete, calcrete nodules, marl and calcified sandstone. Presence of secondary minerals such as siderite, calcite, aragonite, quartz, chalcedony, smectite, chlorite, zeolite, Mg-Fe-Al hydroxides and clay minerals associated with basalt alteration are largely an effect of CO₂ concentration. Fine to medium grained clay, carbonate and quartz-rich matrix occurs at several places. Carbonaceous laminations at several places

are also noticed. White to buff coloured intertrappean limestone beds vary in thickness from few cm. to ~ 8 m, though their lateral continuity is inconsistent, forming lenses and discontinuous beds. At places, limestone circular micritic pellets are also observed. The limestone contains microcrystalline and chalcedonic chert, formed by precipitation of silica saturated hydrothermal solutions. The clay mineral phases in the infra-/inter-trappean beds and weathered Deccan basalt show dominance of montmorillonite, minor amounts of chlorite and illite (Salil, et al., 1994). Association of smectite with the carbonate facies rich in Fe, Mg and Al is observed (Salil, et al., 1996). These rocks show Mg, Fe substitution for Al in smectite (Salil et al., 1997; Shrivastava and Ahmad, 2005). But, clay minerals present in the intra-volcanic bole horizons formed during hiatuses between two volcanic episodes, contain Fe-rich smectite and most of these clays are dioctahedral type, showing a balance between net layer and interlayer charges (Ahmad and Shrivastava, 2007). Kaolinite contains silica in which Fe³⁺ substitutes for Al³⁺ at the octahedral site (Shrivastava, et al., 2012). The secondary minerals formed during low temperature (<150 °C) basalt alteration, occur between the different Deccan volcanic episodes. The mineral assemblages developed depend upon the extent of alteration and temperature that existed at the initial stage of basalt alteration. Primarily, opal/chalcedony/quartz, allophone, kaolinite/halloysite are



Figure 3. Development of carbonate facies between two lava flows - CO₂ sequestration in the past represented by thick limestone and inter-calcarious lithofacies, calcrete, calcified siltstone and marl.

formed, but with increased degree of alteration, formation of more complex smectite, zeolites and carbonates takes place at the expense of SiO₂ rich minerals (Steffansson and Gislason, 2001; Steffansson, 2010). In an environment where high concentration of CO₂, is available, zeolites and clays undergo replacement by the carbonate solid solutions (siderite, dolomite, and magnesite) and quartz (Rogers, et al., 2006). Nature of intercalated weathering and sedimentary horizons are common within continental basalt successions (Widdowson et al., 1997; Jerram, 2002), where, high atmospheric pCO₂ (1110-1850; mean value of 1480 ppmv) often existed during the Deccan volcanic activity [from 70 m. y. (Late Cretaceous period) to 63 m.y. with a major event at 65 ± 0.3 m.y. (Salil, et al., 1997; Chenet, et., 2007; Shrivastava, et al., 2012)] thus, making the possibility of replacement of clays by carbonates highly likely leading to the development of carbonate facies, though these assumptions need to be verified experimentally.

MINERAL CARBONATION REACTIONS AND SEQUENCE OF MINERAL FORMATION

Experimental and natural studies (McGrail et al., 2006; Matter et al., 2007; Oelkers et al. 2008 and Prasad et al., 2009) on basalt-water-CO₂ chemical reactions have concluded that water charged with abundant CO₂ reacts

with basalt and releases the Mg bond of pyroxene and olivine. This in turn combines with the carbonates to form highly stable MgCO₃ (magnesite), whereas water with lower quantity of CO₂ reacts with plagioclase, releases Ca and forms CaCO₃. However, several important issues related to - (a) what fraction of CO₂ is to be injected into the basalts, which would react before it finds its way back to the surface, (b) do the secondary carbonate minerals so formed clog the plumbing and (c) will alteration by-products such as silica, clays, zeolite coat the surfaces and slow down the reaction rate between the CO₂ charged water and the rock (Table 1) remained unanswered.

Aqueous mineral carbonation process enhances the extent of reaction as well as the rate of conversion-activation of the mineral reactants. Mineral activation follows two paths - (a) size reduction to increase relative surface area and (b) destruction or disordering the crystal lattice to form an amorphous material. For carbon sequestration or mineral carbonation, initial studies of O'Connor et al. (2002) consisted of experiments to substantiate carbonation reaction $[(Mg_2SiO_4 \text{ (Olivine)} + 2CO_2 \text{ (Carbon dioxide)} = 2MgCO_3 \text{ (Magnesite)} + SiO_2 \text{ (Silica)} + 54kJ)]$ of natural olivine. The aqueous mineral carbonation reaction sequence includes early-stage precipitation of Mg carbonate, which is co-eval with silicate dissolution. Mani et al. (2008) and Kelemen and Matter (2008) have discussed reactions, wherein CO₂ is stabilized

Table 1. Summary of the experimental data pertaining to effects of CO₂ on the rate of dissolution of silicate minerals (modified after, Golubev et al., 2005)

Minerals	pH	CO ₂ effects	References
Forsterite	4-11	Absent	Golubev et al. (2005)
Olivine (Fo92)	4-6	Absent	Pokrovsky and Schott (2000b)
Olivine (Fo92)	>9	Inhibition	Wogelius and Walther (1991) Pokrovsky and Schott (2000b)
Olivine (Fo92)	10.5-11	Absent	Golubev et al. (2005)
Augite	4	Absent	Brady and Carroll (1994)
Labradorite	3.2 ^a	Absent	Carroll & Knauss (2005)
Anorthite	4	Absent	Brady and Carroll(1994)
Anorthite	5.5-8.5	Acceleration	Berg and Banwart (2000)
Basalt glass	8	Absent	Brady and Gislason (1997)

Table 2. Thermodynamic equilibrium constants at specified temperatures and total pressures of the chemical reactions used to construct the log-log diagram of Ca/Mg activity ratio vs. fugacity.

Reactions	Log K values	
	100°C 1.013 bar	150°C 500 bar
Calcite + Mg ²⁺ + H ₂ O = Brucite + Ca ²⁺ + CO _{2(g)}	-3.3197	-1.6714
Dolomite + Mg ²⁺ + 2H ₂ O = 2Brucite + Ca ²⁺ + 2CO _{2(g)}	-8.0936	-4.9137
Magnesite + H ₂ O = Brucite + CO _{2(g)}	-3.5065	-2.1415
2Calcite + Mg ²⁺ = Dolomite + Ca ²⁺	1.4542	1.5709
Dolomite + Mg ²⁺ = 2Magnesite + Ca ²⁺	-1.0806	-0.6307
2Dolomite + Mg ²⁺ = Huntite + Ca ²⁺	-3.5007	-2.6995
Huntite + Mg ²⁺ = 4Magnesite + Ca ²⁺	1.3395	1.4381
2Calcite + Mg ²⁺ = dis-Dolomite + Ca ²⁺	0.3416	0.6615
Disordered-Dolomite + Mg ²⁺ = 2Magnesite + Ca ²⁺	0.032	0.2787
2Disordered-Dolomite + Mg ²⁺ = Huntite + Ca ²⁺	-1.2755	0.8807

by reacting with olivine [(Mg₂SiO₄ Forsterite/Olivine + 2CO₂ → 2MgCO₃ Magnesite + 2SiO₂ Silica)], pyroxenes [(Fe₂Si₂O₆ Ferrosilite/Pyroxene + 2CO₂ → 2FeCO₃ Siderite + 2SiO₂ Silica)] and plagioclase [(CaAl₂Si₂O₈ Anorthite / Plagioclase + CO₂ + 2H₂O → CaCO₃ Calcium Carbonate + Al₂Si₂O₅(OH)₄ Kaolinite]] and forms the stable carbonate minerals - magnesite, siderite and calcite. Addition of water during mineral carbonation facilitates formation of calcite and magnesite [(Mg₂SiO₄ Mg-olivine + CaMgSi₂O₆ Ca,Mg-Pyroxene + 2CO₂ + 2H₂O → Mg₃Si₂O₅(OH)₄ Serpentine + CaCO₃ Calcite + MgCO₃ Magnesite)], as CO₂ combines with water and forms HCO₃⁻. However, limited work has been carried out on these reactions using P, T, and time variables.

Detailed field and laboratory studies (including modelling under varied, but controlled physical and chemical parameters of near natural conditions) are required to be undertaken on basaltic lava flows in the eastern Deccan volcanic province. Sequestration by mineral carbonation leads formation of solid carbonates, involving dissolution of primary silicates and precipitation of neo-formed phases, mainly carbonates, opaline silica and

clay minerals. Thermodynamic equilibrium constants at particular temperatures and pressures of chemical reactions are summarized in Table 2.

Mineralogical studies of Crovisier et al., (2003) indicate that an alteration layer, primarily of palagonite forms over the surface of basaltic glass in response to chemical attack by water. Under certain conditions, such as prolonged reaction time and high temperature, the alteration layer formed consists of an amorphous gel-like material, leading to the suspicion of hydration of glass due to water permeation and alkali inter-diffusion. In some cases, the alteration layer is crystallized to some extent and contains clay minerals (smectite). Such layers are formed mainly by the process of co-precipitation of the elements dissolved from the basalt. In addition to these hydrated aluminosilicates, hydrated residual glass is also present, formed as a consequence of inter-diffusion processes. In this scenario, an integrated study on carbonation mechanism, mineral paragenesis and application of geochemical codes for modeling is required.

GEOCHEMICAL CODES AND THEIR APPLICATION

Quantification of basalt carbonation and analysis of macrochemical processes require application of geochemical reaction codes that help in simulation of the mineral carbonation products formed during CO₂ sequestration reaction with basalt. A geochemical code is defined as the integration of mathematical expressions, describing theoretical concepts and the thermodynamic relations on which aqueous speciation, oxidation-reduction, precipitation-dissolution, and adsorption-desorption calculations are based. These codes are considered efficient when they encompass all the requisite sub-models and the imperative aqueous complexes, solids and gases for significant elements of preference to interpret a provided data-set adequately. Extensive databases of thermodynamic property values and kinetic rate constants are required for these codes.

Geochemical codes (Cited Table 5.1; Allison et al., 1991) used for speciation and solubility calculations are more pertinent to such work and include- MINTEQA2 (Allison et al., 1991), EQ3/6 (Wolery, 1992), PHREEQC (Parkhurst and Appelo, 1995), REACT (Bethke and Torgersen, 1998) and KINDIS. These chemical reaction codes are divided into two main groups such as (a) aqueous speciation solubility codes and (b) reaction path codes. The former group of codes such as WATEQ, REDEQL, GEOCHEM, MINEQL, MINTEQ, and their later versions have used in the calculation of aqueous speciation/complexation and the degree of saturation of the speciated composition of the aqueous solution with respect to the solids in the code's thermodynamic database. They have also capabilities to calculate mass transfer between a single initial and final state that results from mineral precipitation/dissolution and adsorption/desorption reactions. Besides the above mentioned features, the reaction path codes, such as PHREEQE, PATHCALC, and the EQ3/EQ6 series of codes also permit simulation of mass transfer due to mineral precipitation as a function of reaction progress. Typical applications include modeling of chemical changes associated with the interaction of minerals and groundwater (Delany et al., 1985) as a function of time. At each step of reaction progress, the code calculates the changes or path of mineral and gaseous solubility equilibrium, the masses of minerals precipitated or dissolved to attain equilibrium and the resulting composition of the aqueous solution. The application of geochemical code for modeling of silicate mineral carbonation mechanism is summarized (Fig. 4). The EQ3/6 release 3230B software package is a set of computer programmes and supporting data files / databases - used in the modeling of complex geochemical processes that take place when aqueous solution reacts with basalt silicates and CO₂, due to which new carbonate

minerals are formed. The code PHREEQC (version 2) written in C programming language has been designed to perform a wide variety of low-temperature aqueous geochemical calculations. PHREEQC is based on an ion-association aqueous model. The MINTEQA2 code is used in combination with a thermodynamic database to calculate complex chemical equilibrium among aqueous species, gases & solids and between dissolved and adsorbed states. Theoretically, this code has four sub-models - (a) aqueous speciation, (b) solubility, (c) precipitation/dissolution, and (d) adsorption. It also incorporates a Newton-Raphson iteration scheme to solve the set of mass-action and mass-balance expressions. The geochemical code REACT is a set of software for manipulating chemical reactions, calculating stability diagrams and the equilibrium states of natural waters, tracing reaction processes, modeling reactive transport in one and two dimensions and plotting the results of these calculations. It can integrate kinetic rate, kinetic rate law and simulate the fractionation of stable isotope in a reacting system. The reactive transport model is a groundwater flow transport model coupled to a chemical reaction model. The KINDIS (version 1) programme is used to calculate speciation of the aqueous species and to simulate the irreversible dissolution of minerals and reversible precipitation of secondary phases.

To understand thermodynamics, kinetics and reaction path of minerals formed, parameters such as solubility constant, saturation index, log activity and thermodynamic properties of minerals (Gibbs free energy, enthalpy and entropy) are required to be considered. Geochemical reaction models require thermodynamic data to calculate geochemical reactions associated with CO₂ sequestration. This is an important data requirement for successful application of geochemical reaction modeling for CO₂ sequestration (Marini 2007). The availability of thermodynamic data for CO₂ and carbonate aqueous species and minerals is in the database files used in geochemical reaction models. It is focused on issues related to computer modeling of geochemical reactions associated with CO₂ sequestration in basic igneous rocks such as basalt and peridotite. These codes differ in their ease of use, but can accurately solve the equilibrium assemblage of mineral solubility, within the limits of thermodynamic databases. The quality of the result of each of these codes is directly related to the quality of these databases. These databases facilitate creation of phase diagrams, describing stability of mineral phases as a function of temperature and pressure. The utility of thermodynamic database leads to their incorporation into "user friendly" chemical speciation, reactive path, and reactive transport using computer codes, such as EQ3/6 (Wolery 1983), PHREEQC (Parkhurst and Appelo 1999), and CHESS (Vanderlee et al., 2002). These codes allow rapid calculations of mineral solubility and solute speciation in a variety of geochemical systems. The

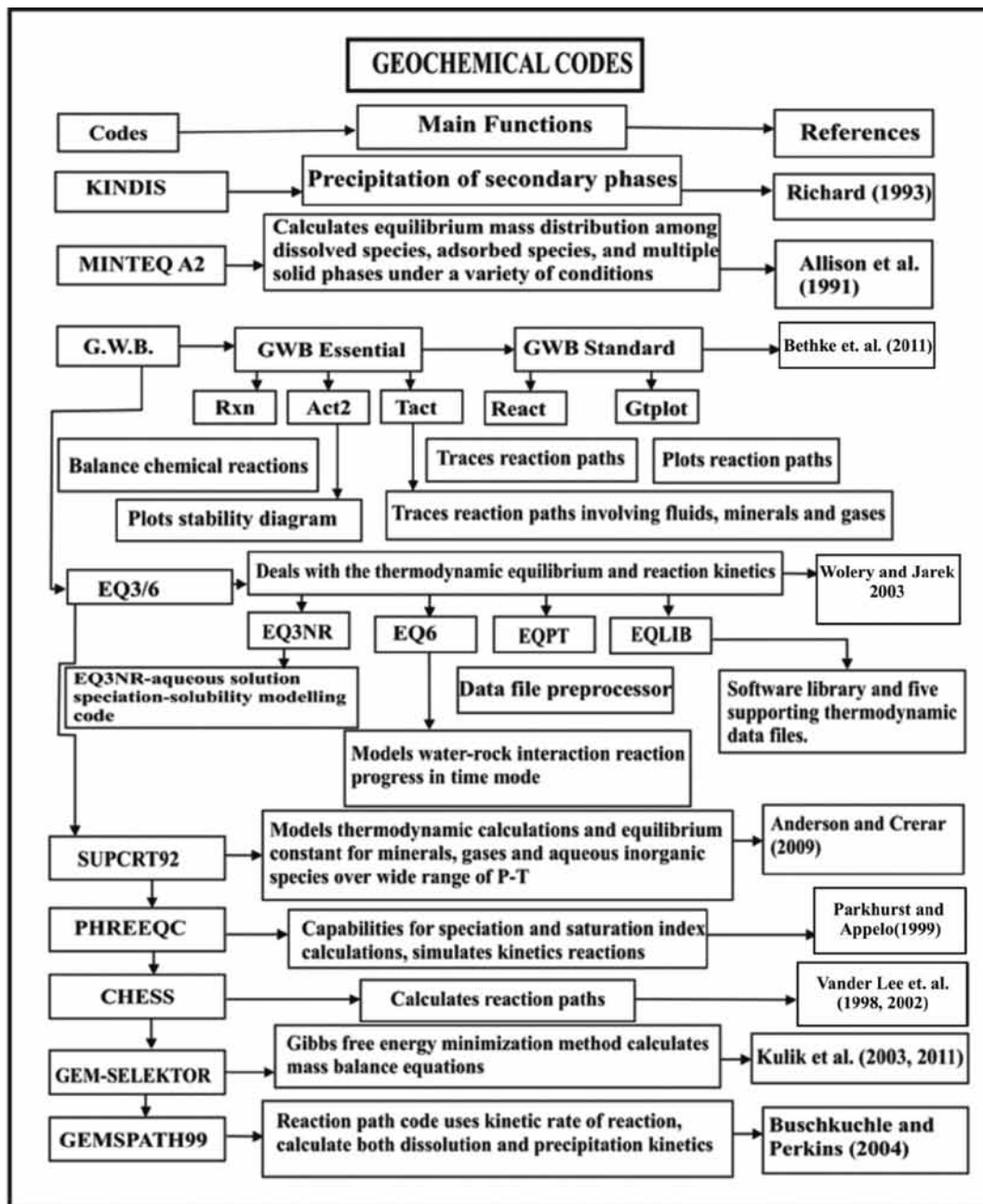


Figure 4. The application of geochemical codes for modeling of silicate mineral carbonation reaction modelling

computer algorithms allow calculation or prediction of the equilibrium state and or the evolution of geochemical systems as a function of reaction progress.

CARBONATION REACTION MODELLING

To predict the course of chemical reaction that takes place during CO₂ sequestration, building of thermodynamic and kinetic model is necessary. Owing to high MgO, CaO contents, the Deccan flood basalt possesses high potential

for CO₂ sequestration, which is further enhanced by the presence of significant amounts of Na₂O and FeO contents. Out of 37 physically and chemically distinct lava flows that occur in the Mandla lobe of eastern Deccan volcanic province, whole rock chemical data for the 4th lava flow (well exposed in the Barasimla and other sections around Jabalpur area) is considered (Table 3) as a starting phase of chemical analysis (cited Fig. 1, 2 and Table 5 from Pattanayak and Shrivastava, 1999 for lava flow location and chemical data, respectively).

Table 3 Composition of basalt (in wt. %)

		Elements	
SiO₂	48.64	Si	17.26
TiO₂	2.83	Ti	0.59
Al₂O₃	14.88	Al	5.51
CaO	10.02	Ca	2.51
Fe₂O₃	14.85	Fe	2.65
K₂O	0.34	K	0.08
MgO	5.77	Mg	2.37
Na₂O	2.77	Na	1.20
P₂O₅	0.19	P	-

- Not considered.

Olivine [chlorophaeite pseudomorphs after olivine; Stokes (1968)], pyroxene, plagioclase, magnetite mineral phases and glass are present in this lava flow. The modal data (for 4th lava flow) determined (on volume percent basis) for pyroxene (Py.), plagioclase (Pl.), magnetite (Ma.), chlorophaeite (Ch.), and glass (Gl.) is 44.75, 40.74, 9.55, 4.75 and 0.25 percent, respectively. These values were multiplied by their respective density values (Py.-3.2, Pl.-2.6, Ma.- 5.2, Ch.-2.6 and Gl.-2.6) to calculate weight percent of pyroxene, plagioclase, magnetite, chlorophaeite and glass, respectively. Mineral phases such as ilmenite and apatite were neglected from subsequent data elaboration because of their low amount and chemical durability. Whole rock composition was recalculated so that the sum of the molar fractions of pyroxene, plagioclase, magnetite, chlorophaeite, and glass is equal to 1. By mass balance calculations, the values obtained for molar fractions (in %) of all the phases of pyroxene, plagioclase, magnetite, chlorophaeite and glass are 0.4600, 0.3387, 0.1575, 0.03972 and 0.00209, respectively. Rock composition was then recomputed assuming that the sum of the molar fractions of minerals is equal to 1. Using major oxide data (Table 2), mineral formulae were calculated for pyroxene [(Ca0.23Mg0.19Fe0.24)Si1.09O3], plagioclase (Ca0.62Na0.25Al1.02Si2.85O8), magnetite (Fe0.28O4), olivine [(Mg0.29Fe0.38)2Si1.66O4], chlorophaeite [(Ca0.47Mg0.38Fe0.49)Fe0.49Si2.15O10(OH)8] and glass (Si0.042Al0.05Fe0.003Mg0.019Ca0.032Na0.013K0.008O3.3) present in this lava flow. Based on mineral formula, cation values (in %) were calculated (Table 4).

The total surface area in contact with water with 1000 ml of water was set to 250cm²/g in the case of Mandla basalt. It was distributed in proportion to the volume percentage of pyroxene, plagioclase, magnetite, chlorophaeite, and glass (Table 4). Their initial amounts in the considered system were calculated through geometric calculations assuming an initial porosity of 0.3. Computer

simulation was performed through EQ3/6 software package of Wolery (1992), maintaining 4936.6 x10⁵ (5 bar pCO₂ pressure) and 9873.2x10⁵ (10 bar pCO₂ pressure) ppmv concentrations of CO₂, specifying the initial surface areas of primary minerals (which are changed by the code in proportion to their remaining masses) and describing their dissolution kinetics (100 - 800 hours for glass, 100-900 hours for plagioclase and 100-1000 hours for pyroxene) at 100 and 200 °C temperatures, respectively. The reaction progress (log Q/K values) obtained for plagioclase, pyroxene and glass (Tables 5a-c) when plotted (Fig. 5a-d) show the formation of carbonate minerals. In the case of plagioclase, the rate of formation of calcite and aragonite is slow at the beginning, but, after 100 hours, reaction rate increases and attains a steady state beyond 1000 hours. In the case of pyroxene (Fig. 5b) and glass (Fig. 5c), the carbonation reaction starts initially at a high rate and there is a slight increase in the rate of formation of calcite and aragonite. However, with progression of time, it lowers down considerably in the case of magnesite, siderite, dolomite and huntite. Standard molar thermodynamic properties for these mineral species were compared with the published values of Gibbs free energy, enthalpy and entropy of formation (Table 6). Values obtained through simulation are significant and considered for the present experimental work.

EXPERIMENTAL WORK

The experiments involved basalt samples in which major oxides (SiO₂= 48.64, TiO₂= 2.83, Al₂O₃=14.88, CaO= 10.02, F₂O₃= 14.85, K₂O= 14.85, MgO=5.77, Na₂O=2.77 and P₂O₅= 10.19) in weight percent were analyzed using XRF technique. To achieve laboratory induced carbonation of silicate minerals under hydrothermal-like conditions and to comprehend the carbonation reaction mechanism, the samples were powdered and passed through 140-170 ASTM sieves and cleaned with deionized water and acetone in an

Table: 4 Mineral formula and cations calculated from major oxides.

Deccan Basalt	Mineral phases and glass				
	Chlorophaeite	Magnetite	Clinopyroxene	Ca-Plagioclase	Glass
Modal % (vol. basis)	4.75	9.55	44.75	40.74	0.25
Densities (g/l)	2.6	5.2	3.2	2.6	2.4
Oxides (wt %)	12.35	49.66	143.2	105.9	0.65
Cations					
Ca	0.00087	-	0.02227	0.016484	0.00002
Mg	0.00069	-	0.0184	-	0.00001
Fe	0.00089	0.0102	0.02324	-	0.0000018
Al	-	-	-	0.02712	0.00004
K	-	-	-	-	0.00001
Na	-	-	-	0.00665	0.0000007
Si	0.0039	-	0.10556	0.07577	0.00003
O	0.01814	0.1472	0.2905	0.21268	0.00201
Mineral Formulae	$(Ca_{0.47}Mg_{0.38}Fe_{0.49})Fe_{0.49}Si_{2.15}O_{10}(OH)_8$	$Fe_{0.28}O_4$	$(Ca_{0.23}Mg_{0.19}Fe_{0.24})Si_{1.09}O_3$	$Ca_{0.62}Na_{0.25}Al_{1.02}Si_{2.85}O_8$	$Si_{0.042}Al_{0.05}Fe_{0.003}Mg_{0.019}Ca_{0.032}Na_{0.013}K_{0.008}O_{3.3}$
Mol. Fract.	0.03972	0.1575	0.4600	0.3387	0.00209

*Modal values given in volume percentages, - = very low values not considered in calculation.

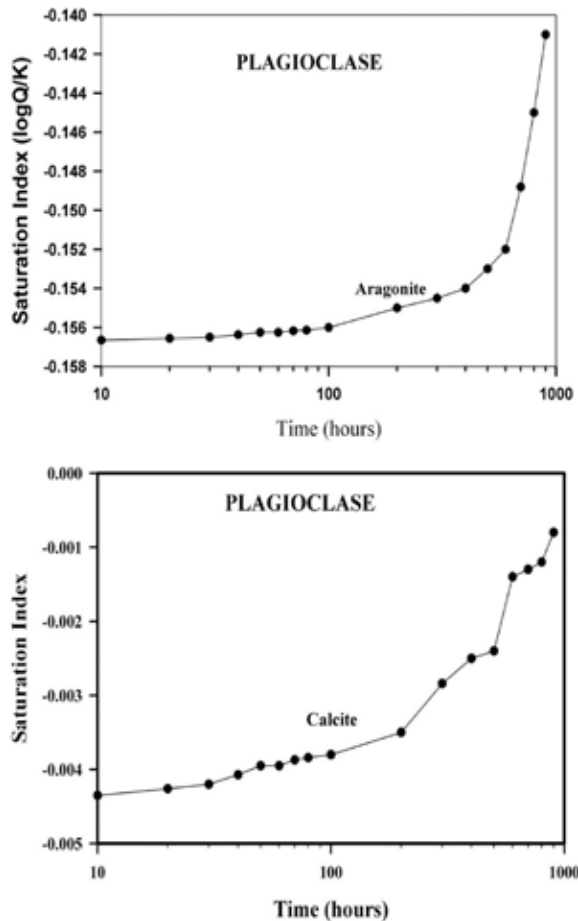


Figure 5a. Time vs. saturation index (log Q/K) data plotted for plagioclase showing formation of calcite and aragonite.

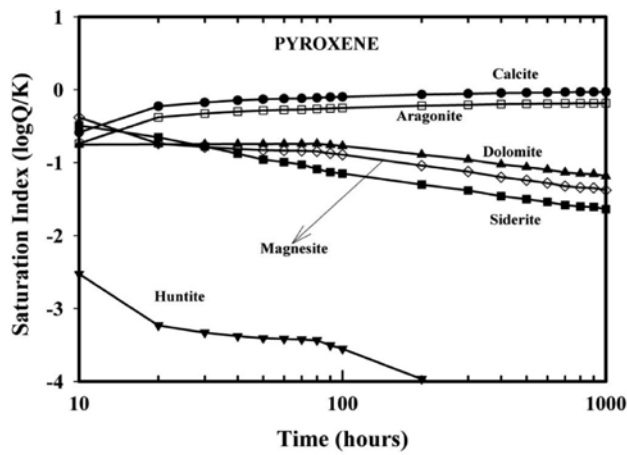


Figure 5b. Time vs. saturation index (log Q/K) data plotted for pyroxene showing formation of calcite and aragonite, magnesite, siderite, dolomite and huntite

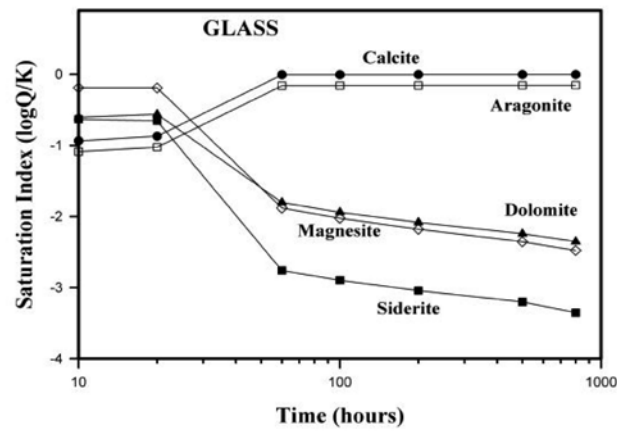


Figure 5c. Time vs. saturation index (log Q/K) data plotted for glass showing formation of calcite and aragonite, magnesite, siderite and dolomite.

Table 5a Reaction progress for plagioclase (at 200°C temperature and 5 bar pressure)

Time (hours)	Aragonite (log Q/K)	Calcite (log Q/K)
10.00	-0.1567	-4.3500e-3
20.00	-0.1566	-4.2600e-3
30.00	-0.1565	-4.2000e-3
40.00	-0.1564	-4.0700e-3
50.00	-0.1563	-3.9500e-3
60.00	-0.1563	-3.9500e-3
70.00	-0.1562	-3.8700e-3
80.00	-0.1561	-3.8400e-3
100.00	-0.1560	-3.8000e-3
200.00	-0.1550	-3.5000e-3
300.00	-0.1545	-2.8400e-3
400.00	-0.1540	-2.5000e-3
500.00	-0.1530	-2.4000e-3
600.00	-0.1520	-1.4000e-3
700.00	-0.1488	-1.3000e-3
800.00	-0.1450	-1.2000e-3
900.00	-0.1410	-8.0000e-4

Table 5b. Reaction progress for pyroxene (at 200°C temperature and 5 bar pressure)

Time (hours)	Aragonite (log Q/K)	Calcite (log Q/K)	Dolomite (log Q/K)	Huntite (log Q/K)	Magnesite (log Q/K)	Siderite (log Q/K)
10.00	-0.7372	-0.5849	-0.7509	-2.5265	-0.3800	-0.4907
20.00	-0.3779	-0.2254	-0.7470	-3.2340	-0.7367	-0.6545
30.00	-0.3268	-0.1742	-0.7460	-3.3306	-0.7865	-0.7773
40.00	-0.2995	-0.1469	-0.7443	-3.3795	-0.8125	-0.8761
50.00	-0.2828	-0.1301	-0.7427	-3.4075	-0.8279	-0.9577
60.00	-0.2766	-0.1239	-0.7419	-3.4170	-0.8334	-0.9936
70.00	-0.2715	-0.1188	-0.7410	-3.4245	-0.8379	-1.0268
80.00	-0.2635	-0.1106	-0.7394	-3.4351	-0.8447	-1.0868
90.00	-0.2544	-0.1015	-0.7567	-3.5045	-0.8714	-1.1313
100.00	-0.2497	-0.0968	-0.7703	-3.5543	-0.8898	-1.1497
200.00	-0.2194	-0.0661	-0.8890	-3.9681	-1.0406	-1.3005
300.00	-0.2076	-0.0541	-0.9572	-4.1939	-1.1216	-1.3816
400.00	-0.1987	-0.0448	-1.0241	-4.4101	-1.1988	-1.4588
500.00	-0.1945	-0.0405	-1.0612	--	-1.2409	-1.5009
600.00	-0.1911	-0.0369	-1.0953	--	-1.2793	-1.5393
700.00	-0.1878	-0.0334	-1.1330	--	-1.3212	-1.5812
800.00	-0.1864	-0.0318	-1.1506	--	-1.3408	-1.6008
900.00	-0.1860	-0.0314	-1.1563	--	-1.3471	-1.6071
1000.00	-0.1843	-0.0296	-1.1838	--	-1.3774	-1.6374

- = data not reproducible

Table 5c. Reaction progress for glass (at 200°C temperature and 5 bar pressure).

Time (hours)	Aragonite (log Q/K)	Calcite (log Q/K)	Dolomite (log Q/K)	Magnesite (log Q/K)	Siderite (log Q/K)
10.00	-1.0879	-0.9356	-0.6042	-0.6317	-0.1868
20.00	-1.0223	-0.8700	-0.5614	-0.6545	-0.1914
60.00	-0.1589	-6.5300e-3	-1.8029	-2.7588	-1.8802
100.00	-0.1570	-4.6700e-3	-1.9399	-2.8974	-2.0254
200.00	-0.1557	-3.2800e-3	-2.0833	-3.0417	-2.1793
300.00	-0.1550	-3.2500e-3	-2.1500	-3.1000	-2.2512
400.00	-0.1548	-3.2418e-3	-2.2089	-3.1519	-2.3098
500.00	-0.1546	-2.2000e-3	-2.2425	-3.2013	-2.3541
800.00	-0.1541	-1.6600e-3	-2.3519	-3.3519	-2.4779

Table 6. Standard molar thermodynamic properties (Holland and Powell, 1998) for mineral and species considered in this study. $\Delta_f G$ is the Gibbs free energy of formation, $\Delta_f H$ enthalpy of formation, S is the entropy, V is the volume; a, b, c are the coefficients of the heat capacity.

Group	Mineral	$\Delta_f G$ KJ/mol	$\Delta_f H$ KJ/mol	S° J/mol/K	V° Cm ³ /mol	a J/mol/K	b J/mol/K	c J/mol/K
Carbonate	Calcite	-1128.81	-2161.51	-1027.74	36.89	140.9	0.5029	-9.50
	Dolomite	-1207.54	-2324.56	-1111.59	64.34	30.89	-0.4905	0.00
	Magnesite	92.50	156	65.10	28.03	186.4	0.00	0.00

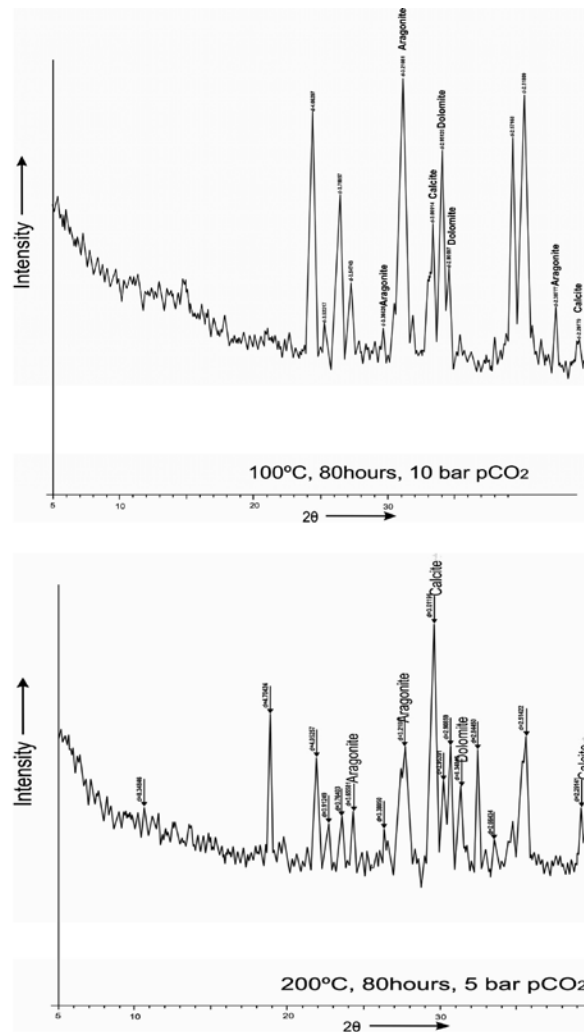


Figure 6. XRD patterns for basalt specimens treated at (a) 100°C temperature and 10 bar pressure and (b) 200°C temperature and 5 bar pressure showing appearance of calcite, aragonite and dolomite.

ultrasonic bath. The calculated (Oelkers and Gislason, 2001) geometric surface and measured BET surface area of a Deccan Traps basalt specimen is 250cm²/g and 23,000cm²/g, respectively. The sequestration experiments were carried out by putting 10 mg each of basalt in 100 ml of deionized water in a Parr Reactor for 50, 60, 70 and 80 hours at 100 and 200 °C temperatures, 5 and 10 bar pCO₂, respectively. The temperature was kept at constant at ± 100 °C and a stirring rate of 100 rpm was applied.

RESULTS AND DISCUSSION

After the experiments, chemical characterization and morphological studies on carbonated basalt specimens was carried out using X-ray Diffraction Analysis (XRD), Raman Spectroscopy and Fourier Transform Infrared Spectroscopy (FTIR) and Scanning Electron Microscope (SEM) mounted with EDS (for compositional determinations of secondary

carbonate minerals). The secondary mineralogy and basalt alteration were identified using X-ray powder diffractograms (XRD). The XRD patterns (Fig. 6) are dominated by the strong intensity peaks of calcite (90.6%), aragonite (75.9%), siderite (32.5%), and dolomite (42.4) at 100 °C and 200 °C for 60 and 80 hours. Calcite, magnesite, siderite, and aragonite have been observed at 100 °C and 5 bar pressure for 70 and 80 hours. Treated specimens were studied using Raman spectroscopic technique to ascertain presence of carbonate ions. It has been found that the characteristic peaks of carbonate ions are at 391.8, 509.7, 665.3 and 1009.6 (Fig. 7). Backscattered electron (BSE) images using SEM photomicrographs of the altered basalt acquired after sequestration experiments indicate that the role of time and temperature is significant. Secondary minerals were identified by SEM-EDS (Fig. 8) and their compositional data (Table 7a-b) obtained by EDS analysis. Based on these results mineral formulae were calculated, which show

Table 7a. Formation of carbonates with progression of time, SEM-EDS data (Specimen-1 treated for 80 hours at 100°C and 5 bars)

Oxides (wt. %)	
CO ₂	14.56
Na ₂ O	2.65
MgO	3.63
Al ₂ O ₃	9.80
SiO ₂	40.95
K ₂ O	0.76
CaO	2.20
TiO ₂	2.21
FeO	22.15
NiO	0.51

Mineral Formulae	
Calcite	Ca _{0.08} C _{0.69} O ₆
Aragonite	Ca _{0.43} C _{1.19} O ₉
Siderite	Fe _{0.64} C _{0.69} O ₆
Magnesite	Mg _{0.28} C _{0.69} O ₆

Table 7b. Formation of carbonates with progression of time, SEM-EDS data (Specimen-2 treated for 80 hours at 100°C and 5 bars)

Oxide (wt. %)	
CO ₂	17.5
Na ₂ O	2.31
MgO	2.39
Al ₂ O ₃	8.62
SiO ₂	43.38
K ₂ O	0.20
CaO	8.17
TiO ₂	1.15
FeO	15.29

Mineral Formulae	
Calcite	Ca _{0.29} C _{0.79} O ₆
Aragonite	Ca _{0.47} C _{1.19} O ₉
Siderite	Fe _{0.45} C _{0.79} O ₆
Magnesite	Mg _{0.11} C _{0.79} O ₆

presence of calcite (Ca_{0.29} C_{0.79} O₆), aragonite (Ca_{0.43} C_{1.19} O₉), siderite (Fe_{0.45} C_{0.79} O₆) and magnesite (Mg_{0.11}C_{0.79} O₆) in the treated samples, though, formation of secondary minerals consisting of clay minerals was not considered during mineral formulae calculations. Present experiments on basalt specimens under varied pressure, temperature and time limits have revealed formation of clay minerals. The clay minerals usually form in high proportions along with the formation of carbonates. Their proportion remains high in a few specimens, which

represent less quantity of carbonate minerals. Thus, it is possible that the clay minerals formed during carbonation process could have slowed down the process of carbonate formation as CO₃ ions trapped within the layered clay structures provide least opportunity for reaction with the freely available Ca, Mg or Fe cations. At 200 °C and 10 bar pressure experiments, the most common carbonate mineral formed is calcite, which suggests a fundamental change in the mobility of elements and secondary mineralogy with an increase of both temperature and pressure.

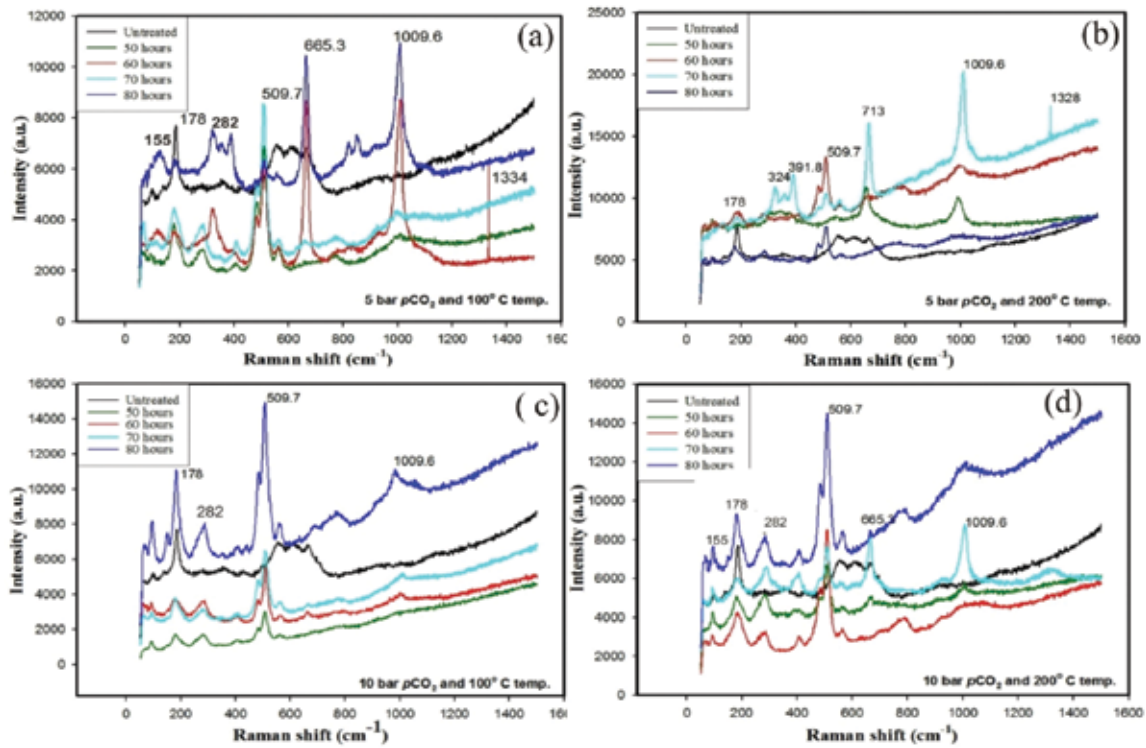


Figure 7. Raman spectra of basalt specimen treated at (a) 100⁰C temperature and 5 and 10 bar pressures, and (b) 200⁰C temperature and 5 and 10 bar pressures showing presence of carbonate peak at 391.8, 509.7, 665.3 and 1009.6 (cm⁻¹).

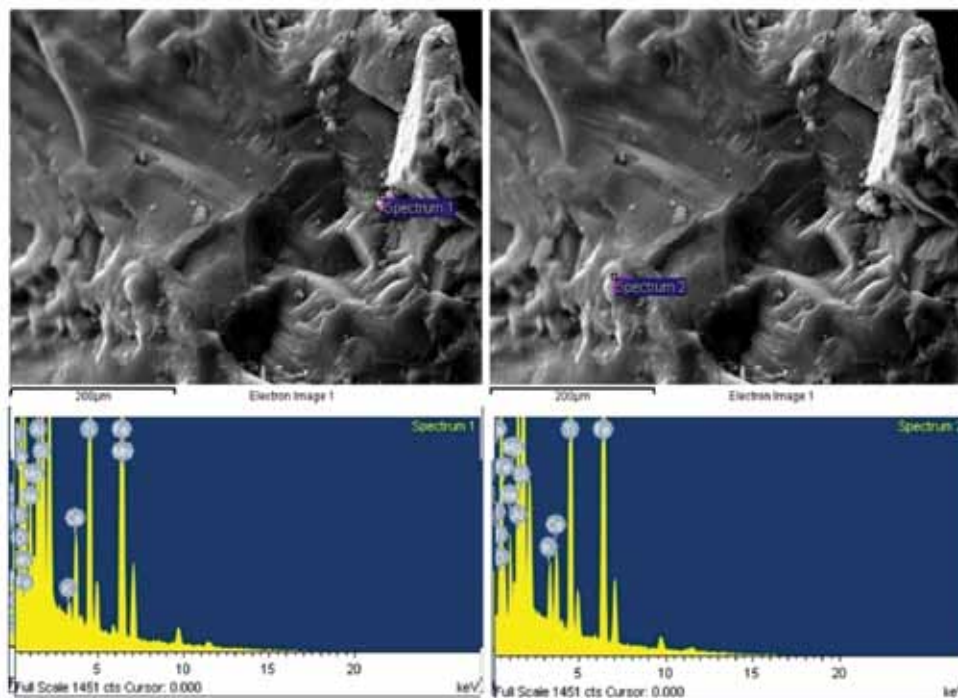


Figure 8. SEM-BSE images of the carbonate minerals formed after treatment of basaltic specimens treated at 100⁰C temperature and 10 bar pressure and (b) 200⁰C temperature and 5 bar pressure with their EDS spectra. Based on major oxide data (obtained after EDS analysis of the specimens) mineral formulae for carbonate minerals were calculated, showing presence of calcite, aragonite and dolomite.

CONCLUSION

The CO₂-water-basalt interaction is studied at 25 – 200 °C as a function of time to evaluate the effects of temperature and extent of reaction during basalt carbonation. Temperature and reaction time, affecting the reaction process is reflected in mineral assemblages, formed in compositional ranges of the basalt and secondary minerals. At 150 – 200 °C, calcite was the only carbonate formed and shows changes with temperature on elemental mobility and secondary mineralogy. Changes with temperature at elevated pCO₂ are reflected in dissolution rate and mechanism, at 200 °C. Dissolution rate is fast and primarily driven by secondary mineral replacement reactions and growth. Formation of the carbonate minerals - calcite, dolomite, aragonite, and siderite takes place largely due to the breakdown of pyroxene, feldspar and glass. However, the discrepancy is evident between thermodynamically calculated mineral species and the experimentally formed carbonate minerals.

ACKNOWLEDGEMENTS

For financial support towards this work, we acknowledge DST Project Grant [No. IS-STAC/CO₂-SR-79/10(G)]. Nishi Rani thanks CSIR for financial support in the form of Research Associateship.

REFERENCES

- Ahmad, M., 2002, Mineralogy and petrogenesis of basalts from Mandla lobe of eastern Deccan volcanic province, India: Unpublished M.Phil Dissertation, University of Delhi, 110 p.
- Ahmad, M. and Shrivastava, J.P. 2008, Compositional studies on clays associated with the intra-volcanic bole horizons from the eastern Deccan volcanic province: palaeo environmental implications. *Memoir Geological Society, India*, v.74, pp 299-321.
- Ahmad, M. and Shrivastava, J.P., 2004, Iron-titanium oxide geothermometry and petrogenesis of lava flows and dyke from Mandla lobe of Eastern Deccan volcanic province, India: *Gondwana Research*, v.2, pp 563-577.
- Allison, J. D., Brown, D.S. and Novo-Gradac, K.J., 1991 MINTEQA2/ PRODEFA2, a geochemical assessment model for environmental systems: version 3.0 user's manual. U.S. EPA, Athens, GA
- Anderson, M.S. and Crerar, D.A., 2009, *Thermodynamics in Geochemistry, the equilibrium model*. New York, Oxford University Press, 588p
- Bachu, S. and Adams, J.J., 2003, Sequestration of CO₂ in geological media in response to climate change-capacity of deep saline aquifers to sequester CO₂ in solution: *Energy Conversion and Management*, v. 44, pp 3151–3175.
- Berg, A. and Banwart, S.A., 2000, Carbon dioxide mediated dissolution of Ca-feldspar: *Chemical Geology* v. 163, pp 25-42
- Bethke, C.M. and Torgersen, T., 1998, Controls on the distribution and isotopic composition of helium in deep ground-water flows: *Geology*, v. 26, pp 291-294
- Bethke, C.M., Sanford, R.A., Kirk, M.F, Jin, Q. and Flynn, T.M., 2011, The thermodynamic ladder in geomicrobiology: *American Journal of Science*, v. 311, pp 183-210
- Brady, P. V. and Gislason S. R., 1997, Seafloor weathering controls on atmospheric CO₂ and global climate, *Geochimica et Cosmochimica Acta*, v. 61, pp 965-973.
- Brady, P.V. and Carroll, S.A., 1994, Direct effects of CO₂ and temperature on silicate weathering: possible implications for climate control: *Geochimica et Cosmochimica Acta*, v. 58, pp 1853-1856.
- Brennan, S. T. and Burruss R. C., 2003, Specific sequestration volumes; a useful tool for CO₂ storage capacity assessment: Open-File Report 03-452 U.S. Geological Survey, Reston, Virginia 20192, 12p.
- Broecker (2008) CO₂ capture and storage: Possibilities and perspectives. *Elements* 4: pp 295-297
- Buschkuehle, B.E. and Perkins, E.H. , 2004, Mineralogy and Geochemical Trapping of Acid Gas in the Edmonton area of Central Alberta, Canada: 7th International Conference on Greenhouse Gas Control Technologies, Elsevier Limited, United Kingdom
- Carroll, S.A. and Knauss, K.G., 2005, Dependence of labradorite dissolution kinetics: *Chemical Geology*, v. 217, pp213-225
- Charan, S.N., Prasad, P.S.R., Sarma, D.S., Archana, K.B., Chavan, C.D. (2010) Evaluation of Deccan continental flood basalts, India for geological sequestration of CO₂ *Jour. of Applied Geochemistry* v. 13, pp.560-565
- Chenet, A. L., Quidelleur, X., Fluteau, F., Courtillot, V., 2007, ⁴⁰K/³⁹Ar dating of the main Deccan Large Igneous Province: Further Evidence of KTB Age and short duration. *EPSL*, v. 263, pp 1-15.
- Crovisier, J.L., Advocat, T. and Dussossoy, J.L., 2003, Nature and role of natural alteration gels formed on the surface of ancient volcanic glasses (natural analogs of waste containment glasses): *Journal of Nuclear Materials* v. 321, pp 91-109
- Delany, J.M., Puigdomenech, I. and Wolery, T.J., 1985, Precipitation kinetics option for the EQ6 geochemical reaction path code: Lawrence Livermore National Laboratory, Livermore, California, UCRL-53642, 44 p.
- Golubev, S.V., Pokrovsky, O.S. and Schott, J., 2005, Experimental determination of the effect of dissolved CO₂ on the dissolution kinetics of Mg and Ca silicates at 25 °C: *Chemical Geology* v. 217, pp 227–238.
- Gysi, A.P. and Stefánsson A. (2012) Experiments and geochemical modeling of CO₂ sequestration during hydrothermal basalt alteration: *Chemical Geology*, v. 306-307, pp10-28.
- Holland, T.J.B. and Powell, R (1998) Internally consistent thermodynamic data set for phases of petrological interest

- J. *Metamorph Geol.* 16: 309-344
- Holloway, S., Garg, A., Kapshe, M., Deshpande, A., Pracha, A.S., Khan, S.R., Mahmood, M.A., Singh, T.N., Kirk, K.L., and Gale, J., 2008, An assessment of the CO₂ storage potential of the Indian subcontinent: *Energy Procedia* 1(1). pp 2607-2613.
- Houghton, R. A. and Wood, G.M., 1987, Global climate change. *Sci. Am.* v. 260, pp 36-44
Lawrence Livermore National Laboratory, Livermore, California
- INTERA (INTERA Environmental Consultants, Inc.). 1983, *Geochemical Models Suitable for Performance Assessment of Nuclear Waste Storage: Comparison of PHREEQE and EQ3/EQ6*. ONWI-473, INTERA Environmental Consultants, Inc., Houston, Texas.
- IPCC, 2005, IPCC Special Report on Carbon Dioxide Capture and Storage. Prepared by Working Group III of the Intergovernmental Panel on Climate Change [Metz, B., Davidson, O., de Coninck, H.C., Loos, M., Meyer, L.A. (Eds.). Cambridge University Press, Cambridge, United Kingdom, New York, NY, USA, 442 p]
- Jerram, D.A., 2002, The volcanology and facies architecture of flood basalts (In press, GSA special publication, Volcanic Rifted Margins).
- Kashyap, M. (2010) Measurements and computation of dispersion and mass transfer coefficients in fluidized beds. Unpublished doctoral dissertation Chicago: Illinois Institute of Technology.
- Kelemen, P. and Matter, J.M., 2008. In situ carbonation of peridotite for CO₂ storage: *Proceedings of the National Academy of Sciences* (in press).
- Kulik, D.A., Wagner T., Dmytrieva S.V., Kosakowski G., Hingerl F.F., Chudnenko K.V., Berner U., 2011, GEM-Selektor geochemical modeling package: revised algorithm and GEMS3K numerical kernel for coupled simulation codes: *Computational Geosciences* v. 17, pp 1-24.
- Kulik, D., Berner, U., Curti, E., 2003, Modelling chemical equilibrium partitioning with the GEMS-PSI code. In: *PSI Scientific Report 2003/ v. 4, Nuclear Energy and Safety* (edited by B. Smith and B. Gschwend), PSI, Villigen, Switzerland, pp. 109-122, 2004
- Mani, D., Charan, N.S., Kumar, B., 2008, Assessment of carbon dioxide sequestration potential of ultramafic rocks in the greenstone belts of southern India: *Current Science*, v. 94, pp 5-60.
- Marini, L. 2007, *Geological Sequestration of Carbon Dioxide: Thermodynamics, Kinetics, and Reaction Path Modeling*: Elsevier, Amsterdam, 470 p.
- Matter, J.M., Takahashi, T. and Goldberg, D., 2007, Experimental evaluation of in situ CO₂-water-rock reactions during CO₂ injection in basaltic rocks. Implications for geological CO₂ sequestration: *Geochemistry, Geophysics, Geosystems* 8: doi 10.1029/2006GC001427
- McGrail, B.P., Schaef, H.T., Ho, A.M., Chien, Y.J., Dooley, J.J. and Davidson, C.L., 2006, Potential for carbon dioxide sequestration in flood basalts: *Journal of Geophysical Research* 111: B12201.
- Metz, B., Davidson, O., de Coninck H., Loos, M. and Meyer L., 2005, IPCC Special Report on Carbon Dioxide Capture and Storage: Cambridge University Press, New York,
- O'Connor, W.K., Dahlin, D.C., Nilsen, D.N., Gerdemann, S.J., Rush, G.E., Penner, L.R., Walters, R.P., Turner, P.C., 2002, Continuing studies on direct aqueous mineral carbonation for CO₂ sequestration: The Proceedings of the 27th International Technical Conference on Coal
- Oelkers, E. H. and Gislason, S.R., 2001, Mechanism, rates, and consequences of basaltic glass dissolution: II. An experimental study of the dissolution rates of basaltic glass as a function of pH and temperature: *Geochimica et Cosmochimica Acta*, v. 67, pp 3817-3832,
- Oelkers, E.H., Cole, D.R., 2008, Carbon dioxide sequestration: A solution to a global problem. *Elements*, v. 4: pp 305-310
- Oelkers, E.H., Gislason, S.R. and Matter, J., 2008, Mineral Carbonation of CO₂: *Elements*, v. 4, pp 331-335.
- Parkhurst, D.L., 1995, User's guide to PHREEQC A computer program for speciation, reaction-path, advective-transport, and inverse geochemical calculations: U.S. Geological Survey Water-Resources Investigations Report 95-4227, 143 p
- Parkhurst, D. L., Appelo, C.A.J., 1999, User's guide to PHREEQC (Version 2) - A computer programme for speciation, batch reaction, one dimensional transport and inverse geochemical conditions. U.S. Geological Survey Water-resources Investigation Report 99 - 4259, 312 p.
- Pattanayak, S.K., Shrivastava, J.P., 1999, Petrography and major-oxide geochemistry of basalts from the Eastern Deccan Volcanic Province, India: West Volume. *Geological Society of India, Memoir*, v. 43 (1), pp 233-270.
- Pokrovsky, O.S. and Schott, J., 2000b, Kinetics and mechanism of Forsterite dissolution at 25°C and pH from 1-12: *Geochimica et Cosmochimica Acta*, v. 64, pp 3313-3325.
- Prasad, P. S. R., Srinivasa Sarma D., Sudhakar, L. Basavaraju, U., Singh, R. S., Zahida Begum, Archana, K. B., Chavan C. D. and Charan S. N. (2009) Geological sequestration of carbon dioxide in Deccan basalts: preliminary laboratory study. *Current Science*, v.96, pp.288-291
- Retallack, G. J. (2002) Carbon dioxide and climate over the past 300 Myr: *Philosophical Transactions of the Royal Society of London*, v. 360, pp 659-674.
- Rochelle, C.A., Czernichowski-Lauriol, I., and Milodowski, A.E., 2004, The impact of chemical reactions on CO₂ storage in geological formations: a brief review. in: *Geological Storage of Carbon Dioxide*, S.J. Baines and R.H. Worden eds., Special Publication of the Geological Society of London v. 233, pp. 87-106.
- Rogers, K.L., Neuhoﬀ P.S., Pedersen A.K. and Bird D.K., 2006, CO₂ metasomatism in a basalt-hosted petroleum reservoir, Nuussuaq, West Greenland. *Lithos* v. 92, pp 55-82.
- Salil, M.S., Pattanayak, S.K., Shrivastava, J.P. and Tandon, S.K.,

- 1994, X-Ray diffraction studies on the clay mineralogy of infra (Lameta)/ inter-trappean sediments and weathered Deccan basalt from Jabalpur, M.P. implication for the age of Deccan volcanism: *Journal Geological Society India*, v. 44, pp 335-337.
- Salil, M.S., Pattanayak, S.K., Shrivastava, J.P., 1996, Composition of smectites in the Lameta sediments of central India: implications for the commencement of Deccan volcanism: *Journal of the Geological Society of India* v. 47, pp 555-560
- Salil, M.S., Shrivastava, J.P., Pattanayak, S.K., 1997, Similarities in the mineralogical and geochemical attributes of detrital clays of Maastrichtian Lameta beds and weathered Deccan basalt, central India: *Chemical Geology* v. 136, pp 25-32.
- Shrivastava, J. P. and Pattanayak S.K., 2002, Basalt of the Deccan volcanic province, India: *Gondwana Research*, v.5, 3, pp 649-665
- Shrivastava, J. P. Mansoor Ahmad and Surabhi Srivastava, 2012, Microstructures and compositional variation in the intra-volcanic bole clays from the eastern Deccan volcanic province: palaeoenvironmental implications and duration of volcanism: *Journal Geological Society of India* v. 80, pp 177-188
- Shrivastava, J.P. and Ahmad, M., 2005, A review of research on Late Cretaceous volcanic sedimentary sequences of the Mandla lobe: implications for Deccan volcanism and the Cretaceous/Palaeogene boundary: *Cretaceous Research*, v. 26, pp 145-156
- Shrivastava, J.P. and Ahmad, M., 2005a, A review research on late cretaceous volcanic sedimentary sequences of the Mandala lobe: Implications for Deccan volcanism and the Cretaceous/Palaeogene boundary: *Cretaceous Research*, v. 26, pp 145-156
- Shrivastava, J. P., Mahoney J. J., and Kashyap, M. R. (2014) Trace elemental and Nd-Sr-Pb isotopic compositional variation in 37 lava flows of the Mandla lobe and their chemical relation to the western Deccan stratigraphic succession, *India Miner. Petrol.*, (DOI 10.1007/s00710-014-0337-3) pp 1-17
- Steffansson, A. and Gislason S. R., 2001, Chemical weathering of basalts, SW Iceland: Effect of rock crystallinity and secondary minerals on chemical fluxes to the ocean: *American Journal Science* v. 301, pp 513-556.
- Steffansson, A., 2010, Low-temperature alteration of basalts – the effects of temperature, acids and extent of reaction on mineralization and water chemistry. *Jokull* v. 60, pp 165-184
- Stokes, W.L., 1968, Relation of fault trends and mineralization, eastern Great Basin, Utah: *Economic Geology* v. 63, pp 741-759.
- Van der Lee, J., 1998, Thermodynamic and mathematical concepts of CHESSE, Ecole des Mines de Paris - Centre d'Informatique Géologique - LHM/RD/98/39: Fontainebleau.
- Van der Lee, J., De Windt, L., Lagneau, V., Goblet, P., 2002, Module-oriented modeling of reactive transport with HYTEC: *Computational Geoscience*, V. 29, pp 265-275.
- van der Lee, S., and Frederiksen, A., 2005, Surface wave tomography applied to the North American upper mantle, in Levander, A., and Nolet, G., eds., *Seismic data analysis and imaging with global and local arrays: American Geophysical Union Geophysical Monograph* v. 157, pp 67-80.
- Widdowson, M., Walsh, J.N. and Subbarao, K.V., 1997, The Geochemistry of Indian bole horizons: Palaeoenvironmental implication of Deccan Intra-volcanic Palaeosurface: *Geological Society London*, v. 120, pp 269-281.
- Wogelius, R.A. and Walther, J.V., 1991, Olivine dissolution at 25C: Effects of pH, CO₂ and organic acids: *Geochimica et Cosmochimica Acta*, v. 55, pp 943-954.
- Wolery, T. J., 1983, EQ3NR, a Computer Program for Geochemical Aqueous Speciation-Solubility Calculations: User's Guide and Documentation. UCRL-53414. Lawrence Livermore National Laboratory
- Wolery, T. and Jarek, R.L., 2003, Software user's manual, EQ3/6, Version 8.0, 10813-UM-8.0-00, Sandia National Laboratories, Albuquerque, New Mexico.
- Wolery, T.J., 1992, EQ3/6, A Software Package for Geochemical Modeling of Aqueous Systems (Version 7.0). Lawrence Livermore Laboratory, Work Report UCRL-MA-110662 PT 1-4.
- Xu, T., Apps J. A. and Pruess K., 2004, Numerical simulation of CO₂ disposal by mineral trapping in deep aquifers. *Applied Geochemistry*, v. 19, pp 917-936.